Solvation Behavior of Gold Nanorods in Water: A Monte Carlo Simulation Study

H. Esfandiar[1], S. M. Hashemianzadeh[2,*], S. Saffary[1] and S. Ketabi[3]

* *e.hashemianzadeh@gmail.com*

[1] **School of Metallurgy and Materials Engineering, Iran University of Science and Technology, Tehran, Iran.**

[2] **Molecular Simulation Research Laboratory, Department of Chemistry, Iran University of Science and Technology, Tehran, Iran.**

[3] **Department of Chemistry, East Tehran Branch, Islamic Azad University, Tehran, Iran.**

Abstract: Gold nanoparticles have become common in many applications of biotechnology due to their specific properties. Shape and size are important attributes which affect their solubility in water. In this study, the outcomes of Monte Carlo Simulation for the solvation of gold nanorods in aqueous solution with the different radii, in terms of solvation free energy, are discussed. Simulation results show a negative solvation free energy for all the samples with radii of 4 to 9Å. The results show that the absolute values of solvation free energy for gold nanorods with smaller radius are larger, which indicate the dependency between the gold nanorods solvation and their radius.

Keywords: Gold Nanorod, Monte Carlo Simulation, Solvation, Free energy.

1. INTRODUCTION

Over the last decades, gold nano particles (GNP) applications have become a focal center of interest [1]. Various properties such as biocompatibility, non cytotoxic effects, optical and electrical properties, which are basically stems from their availability in different sizes and forms (rod, tube, sphere, shell, cage, etc.); have made GNPs appropriate candidate for many applications [2]. Rendering high surface area at nanoscale leads to utilizing GNPs in cancer therapy [3, 4], drug transportation [5, 6], imaging [7, 8], and biological disclosure and diagnosis [9, 10]. Previous studies showed that surface adsorption of GNP has direct effect on both dynamic behavior of the nanoparticles and the configuration of the molecules which are adsorbed on the surface of GNP [11]. In this case, solubility limitation has been one of the most controversial threats for all nanomaterials. Among all possible alternatives for GNPs, gold nanorods (GNRs) have caught special attention because of their vast surface area [12].

Restrictions of experimental studies on nanoparticles especially in such small-scale begets using computational simulation as an feasible approach to study these systems [13]. One of the enthralling subjects is investigation of the adsorption mechanism of water molecules on the spherical gold nanoparticles by means of molecular dynamic (MD) simulation. Recent reported studies revealed that decreasing the diameter of GNPs not only increases the water adsorption, but also decreases average interaction energy per a water molecule. Moreover, oxygen and hydrogen atom distribution patterns showed that the adsorption of water molecules arises in two water shell-like structures close to the GNPs surface [14]. Additionally, arrangement and self-diffusion coefficient of water molecules confined between two gold plates of (001) planes separated by different gap sizes and the arrangement of water molecules inside gold nanotubes of various diameters have been studied via MD simulation. According to their research, the interaction energy between water molecule and Au nanotube enlarges as the nanotube diameter reduces and the diffusing ability of water molecules is enhanced when they are contained within smaller Au nanotubes [15, 16].

In this study, the solubility of GNRs with

different radii has been investigated to evaluate the size effect on solvation. Monte Carlo simulation and perturbation methods are used to calculate solvation free energies and compare solubility of these nanorods. In addition arrangement of water molecules surrounding GNRs is studied through reduced density profile of water molecules to compare GNRs' solvation.

2. COMPUTATIONAL DETAILS

Monte Carlo (MC) simulation is carried out for six GNRs in water media using standard procedure of Metropolis sampling including 107 configurations [17]. To scale the temperature of the water molecules and the Au atoms to equilibrium temperature of 298 K in the course of the simulation Canonical ensemble is utilized. The simulation box was defined with $40 \times 40 \times 56$ Å³ dimensions and periodic boundary conditions imposed in x, y and z directions, and a relative cutoff of 12 Å. The box contains about 1000 water molecule surrounding gold nanorods of 72, 168, 200, 296, 360 and 488 Au atoms which radii vary from 4 to 9Å with the same length of 32Å. Dimensions of GNRs is chosen in accordance to the periodicity of a fcc gold with the lattice constant of 4.07Å, and the Au atoms are cut from a fcc Au crystalline so that the axis of the GNRs is parallel to the [100] direction (Fig. 1). Using a dilute solution; one molecule of GNR is merged in a rectangular box of water. The simulation data should be properly analyzed to extract applicable properties. To verify accuracy of Monte Carlo calculations, statistical fluctuations of ensemble averages are calculated. The statistical errors which reported as standard deviations are under1%.

The intermolecular interaction energy (E_{inter}) encompasses two parts of water–water and gold–water potentials. The transferable intermolecular potential function (TIP3) [17,18] is applied for modeling water molecules. The interactions between GNRs and the water molecules are characterized by site-site interaction potential with parameters ε_i and σ_i for each atom:

$$E_{ij}^{AB} = 4\epsilon_{ij}\left[\left(\frac{\sigma_{ij}}{r_{ij}}\right)^{12} - \left(\frac{\sigma_{ij}}{r_{ij}}\right)^{6}\right] + \frac{q_i\, q_j\, e^2}{r_{ij}} \qquad (1)$$

ε_{ij} and σ_{ij} are calculated based on the Lorentz–Berthelot combining rules [19]. The LJ parameters for the Au atoms are derived from the universal force field (UFF) [20] with the quantity of 0.039 kcal.mol^{-1}(ε) and 2.934 Å (σ).

Free Energy Perturbation (FEP) approach is used to investigate the solvation free energies of GNRs in water. The free-energy difference between two states 0 and 1 can be given by [21].

$$\Delta A_{0 \to 1} = A_1 - A_0 = -k_B T \ln\left\langle \exp-(H_1 - H_0)/k_B T \right\rangle_0 \qquad (2)$$

where k_B is the Boltzmann constant and $H_1 - H_0$ is the difference in the Hamiltonian of systems 0
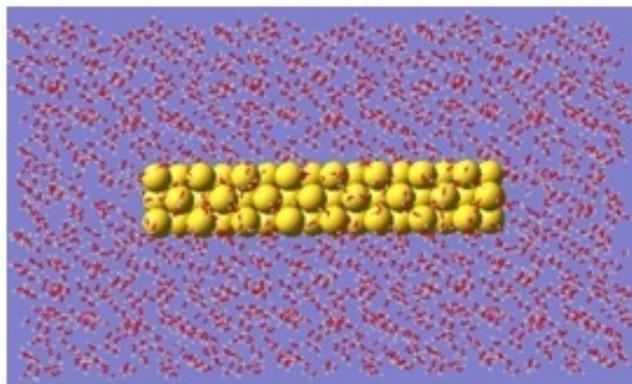

Fig.1. Schematic diagram of the simulation box with periodic boundary condition imposed in all directions.

and 1. Since the kinetic energy contributions is possible to be integrated out in the Helmholtz free energies calculation, the difference in the Hamiltonian can be resulted from potential energy [22]. Hence, the FEP formula for the Helmholtz free-energy difference between two systems 0 and 1 is as follows:

$$\Delta A_{0 \to 1} = A_1 - A_0 = -k_B T \ln \langle \exp - (U_1 - U_0)/k_B T \rangle_0 \quad (3)$$

Therefore $U_1 - U_0$ represents difference in the potential energy of states 0 and 1. It must be considered that if the two states of 0 and 1 do not overlap in phase space, the energy differences between the two states will be much larger than $k_B T$, so the value of the potential energy variations between the two states will not be very accurate. In this case, a coupling parameter λ is introduced to divide the intervals 0–1 into n subintervals. Then, a combination of solute and solvent's LJ parameters in the intermediate states between 0 ($\lambda = 0$) and 1 ($\lambda = 1$) can be written by

$$\varepsilon_\lambda = \lambda \varepsilon_1 + (1 - \lambda)\varepsilon_0, \quad (4)$$

$$\sigma_\lambda = \lambda \sigma_1 + (1 - \lambda)\sigma_0 \quad (5)$$

In this work, both $\varepsilon_0 = 0$ and $\sigma_0 = 0$ correspond to the initial state, where there is no interaction between solute and solvent. Then, the total Helmholtz free-energy difference between 0 and 1 states can be obtained through taking a summation of these averages,

$$\Delta A_{0 \to 1} = \sum_{\lambda=0}^{\lambda=1} \Delta A_\lambda = \sum_{\lambda=0}^{\lambda=1} -k_B T \ln \langle \exp - (U_{\lambda'} - U_\lambda)/k_B T \rangle_\lambda \quad (6)$$

The solvation free energy stands for the needed free energy to transfer one mole of solute (B) from an ideal gas state to an infinitely dilute solution. This free energy is the difference between the free energies of solute B in the aforementioned two phases:

$$\Delta A_{solv}(B) = A_{solv}(B) - A_{gas}(B) \quad (7)$$

Using FEP method, the solvation free energy of the species B (which in this investigation is GNR), can be interpreted in terms of perturbations where the species approaches to zero in the gas phase and in solution.

$$\Delta A_{solv}(B) = \Delta A_{gas}(B \to 0) - \Delta A_{solv}(B \to 0) \quad (8)$$

3. RESULTS AND DISCUSSION

Water molecules arrangement surrounding GNRs affected by water-gold interaction is shown via reduced density profile of oxygen atoms. In addition variation of solvation free energy with alteration of radius of GNRs is investigated.

Radial distribution functions (RDF), g(r), measure the probability of finding a particle as a function of distance from GNRs (local density) relative to that expected from a completely uniform distribution.

Local density for solvent atom type x, ρ_x (r) is obtained from the frequency histogram using:

$$\rho_x(r) = \frac{n_x(r)}{dv} \quad (9)$$

where, n_x (r) is the frequency of finding an atom of type x (oxygen or hydrogen) between r and r+dr of the central axis of GRNs [23].

Fig. 2 shows the reduced density profiles of oxygen atoms surrounding GNRs. Since the mass center for water molecule is located close to its oxygen atom. Oxygen reduced density profile is used to represent water molecule reduced density profile. The vertical axis indicates the reduced density (ρlocal /ρbulk). ρlocal stands for number of oxygen that their center forms a cylindrical shell with the same axis of the GNRs, divided by the shell volume, where the horizontal axis represents distance of oxygen atoms from the surface of GNRs. To clarify the influence of GNRs radius on water molecules distribution, reduced density profiles are shown for different radii. It can be seen that all of the density profiles are showing peaks corresponding with the shell-like formations of water molecules around the surface of GNRs.
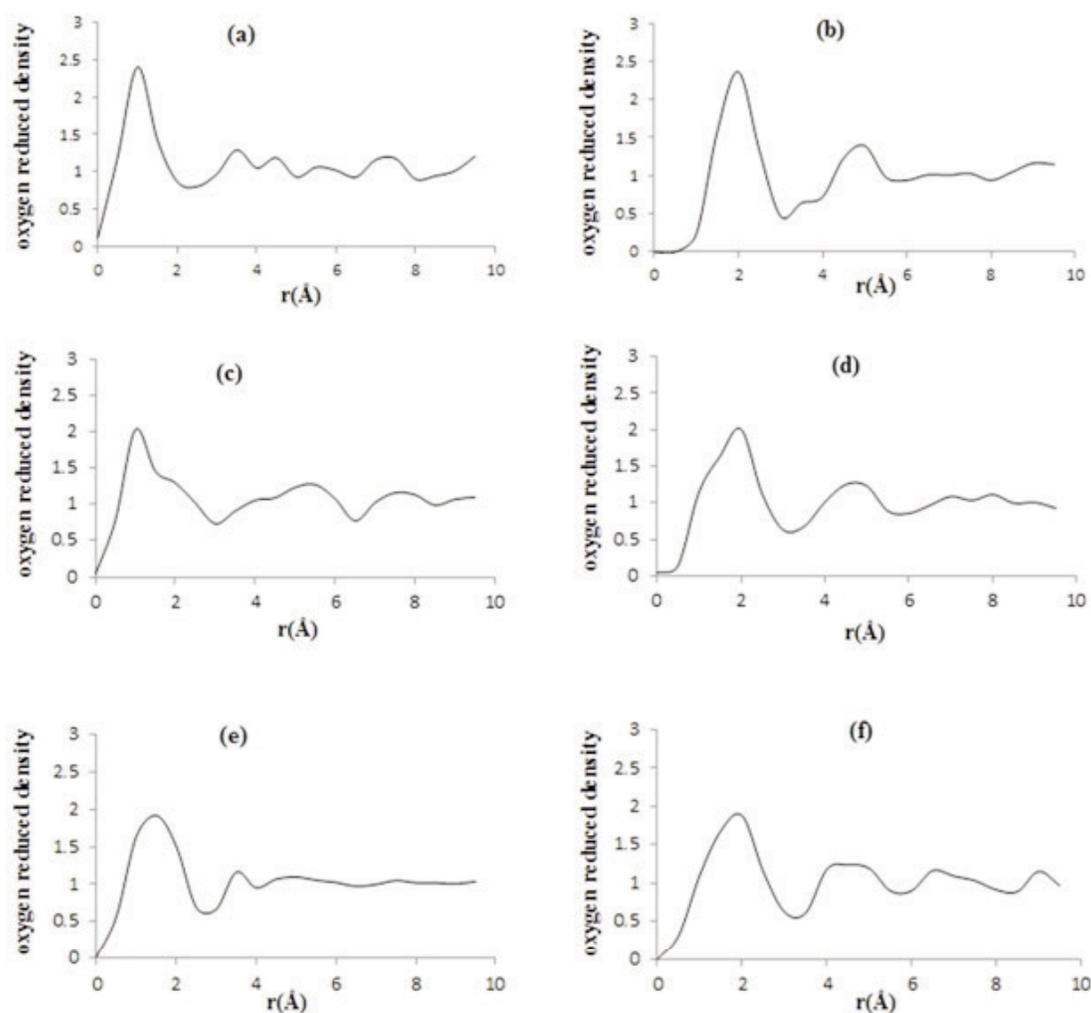
Fig. 2. Oxygen reduced density profiles around GNRs with radius of: (a) 4Å, (b) 5Å, (c) 6Å, (d) 7Å, (e) 8Å, and (f) 9Å.

As it is shown in Fig. 2, the first peak takes place within 3Å of the GNRs surface, in which the potential energy, caused by the intermolecular interactions between the water molecules and the Au atoms, has the lowest value. By increasing the distance from the GNRs surface, this potential energy first escalates and forms an energetically unfavorable region for the accommodation of water molecules in the distance between the first two peaks. The second peak, appearing at approximately 4Å from the GNRs surface, is caused by increasing the appealing part of the potential energy. From this point onwards, broad and connected peaks are provided due to the hydrogen bonding of some water molecules

within the shells. In all samples, adopting the water molecules to a bulk structure at distances greater than 8Å from the GNRs surface demonstrates the limit of bulk behavior for water. To have an analogy of water arrangement around GNR, a snapshot issued from the simulation GNR with radius of 8 Å is given in Fig. 3. This top view picture shows the arrangement of the first layer of water molecules around the GNR which presents a cylindrical symmetry of the water environment near to the GNR.

Variation of first peak height of oxygen reduced densities as its maximum value, and local density of water molecules within 4 Å (ρlocal 0-4) with GNRs' radius are compared in
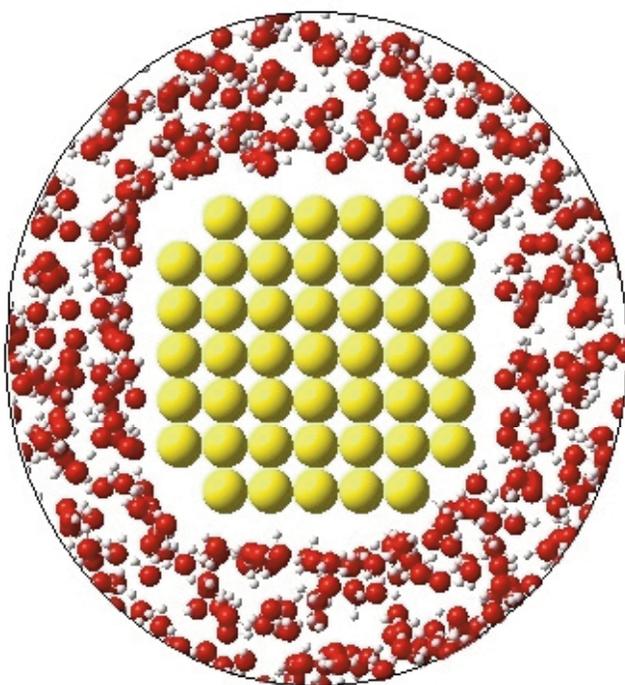
Fig. 3. Cylindrical symmetry of water molecules around GNR

Table 1. ρlocal 0-4 is calculated by dividing the number of water molecules within 4 Å of the GNRs surface by volume of this area. In other words, ρlocal 0-4 is equal to area below the first peak of the reduced density profiles. Regarding to Table 1, ρlocal 0-4 and the first peak height rises as GNRs' radius become smaller, which means configuration of water molecules around

Table 1. Variation of first peak height of oxygen reduced densities and water molecules local density within 4Å (ρlocal0-4) with GNRs' radius.

GNRs radius (Å)	E_{inter}(kcal/mol)	ΔA_{solv} (kcal/mol)
4	-17.876	-86.653
5	-16.990	-72.786
6	-14.337	-48.046
7	-11.339	-25.176
8	-11.235	-23.292
9	-11.190	-21.446

narrower GNRs is more packed. This may also be concluded from Fig. 2, that with increasing radius of GNR, the first peak becomes shorter and wider.

Table 2. shows the list the intermolecular interaction energies (E_{inter}) of all samples as the radius of GNRs, respectively. E_{inter} is explained previously as sum of the energy contributions from water–gold and water–water interactions. Since the LJ parameters for hydrogen atoms in TIP3 model are zero, the water–gold interaction includes only vander Waals interaction between gold and oxygen atoms. Moreover, portion of water–water interaction does not change with GNRs radius, so the difference between E_{inter} values stems from only change of water–gold interaction. The results affirm that absolute value of E_{inter} decreases with increasing the GNRs radius, which is in agreement with the ρlocal 0-4 and reduced density values of Table 1. In fact, greater water–gold interaction energy for smaller GNRs results in a more packed arrangement of water molecules in the rods' vicinity.

Solubility of spherical gold nanoparticles

agrees with the present results [13]. Based on this consequence, smaller gold nanoparticles have stronger interaction with surrounding water molecules, which the lower cohesive energy of surface Au atoms for smaller particles is considered to be the main reason. The ratio of number of surface atoms and bulk atoms in Au nanoparticles of smaller size is greater than ratio in larger nanoparticles. Hence, cohesive energy is reduced and a more unstable structure occurs. Accordingly, these surface atoms have a greater tendency to absorb water molecules to increase their cohesive energy. Results also show that the influence of cohesive energy becomes less significant as nanoparticle diameter increases. As it is shown in Table 2, E_{inter} values do not decrease monotonically, and the radius 7Å is a critical size from which the declining trend levels off.

Solvation-free energy (ΔA_{solv}) is computed as aforementioned discussion in computational details. The fluctuation of solvation-free energies with GNRs radius is presented in Table 2. ΔA_{solv} value is negative for all the GNRs, which conveys the hydrophilic nature of gold particles. In addition, its absolute value decreases as the radius of GNR increases, which indicates the higher solubility potential for the narrower GNRs. It can be seen in Tables 1 and 2 that the variations of ΔA_{solv} and Einter values with GNRs radius are the same and their declining trend levels off after 7Å for radius. Actually from this radius onwards, influence of increasing the radius on degree of solubility is not significant and this comes from the change in hydrogen bonding structures.

The trend of decreasing of solvation free energy with growing of nanorod's radius will be reversed if the structure is hallowed. It has been shown that solvation free energies of Multi-Walled Carbon Nanotube (MWCNTs) in water environment increase with growing the MWCNTs diameter [24]. In fact, unlike solid structures like rod, in a hallow structure such as (MWCNTs) with constant number of walls; the ratio of atoms presenting at the surface to the bulk atoms is constant. Therefore the cohesive energy of surface atoms on MWCNTs doesn't altered with MWCNTs size and so the greater solubility of larger MWCNTs (in diameter or

Table 2. Intermolecular interaction energy (E_{inter}) and Solvation-free energy (ΔA_{solv}) of GNRs.

GNRs radius (Å)	E_{inter}(kcal/mol)	ΔA_{solv} (kcal/mol)
4	-17.876	-86.653
5	-16.990	-72.786
6	-14.337	-48.046
7	-11.339	-25.176
8	-11.235	-23.292
9	-11.190	-21.446

length) stems from their larger interacting surface area with solvent.

4. CONCLUSION

In this study, Monte Carlo Simulation method is utilized to investigate the solubility of GNRs with radii in a range of 4 to 9 Å. Results affirm that water molecules arrange in a shell-like structure around the GNRs, and greater gold-water attraction energy for narrower GNRs leads to a more packed water distribution around their surface.

Variation of solvation free energy (ΔA_{solv}) with GNRs radius showed that hydrophilicity and solubility potential declines as the radius grows. This is caused by cohesive energy change of surface atoms. Furthermore, the trend of solvation free energy (ΔA_{solv}) of GNRs with increasing the diameter is opposite to that of previous studies for hallow nanostructures like CNTs, due to variation of interacting surface area. According to the results, narrower GNRs represent higher solvation potential and build more stable particles in water. The matter of stability is a main concern in bio or non-biomedical applications for nanomaterials.

REFERENCES

1. Jain, S., Hirst, D. G. and O'Sullivan, J. M., Gold nanoparticles as novel agents for cancer therapy., Br. J. Radiol., 2012, 85, 101–13.
2. Brust, M. and Kiely, C. J., Some recent

advances in nanostructure preparation from gold and silver particles: a short topical review", Colloids Surfaces A Physicochem. Eng. Asp., 2002, 202, 175–186.

3. Sun, T. M., Wang, Y. C., Wang, F., Du, J. Z., Mao, C. Q. and Sun, C. Y., "Cancer stem cell therapy using doxorubicin conjugated to gold nanoparticles via hydrazone bonds.", Biomaterials., 2014, 35, 836–45.

4. Ahmad, M. Z., Akhter, S., Rahman, Z., Akhter, S., Anwar, M. and Mallik, N., "Nanometric gold in cancer nanotechnology: current status and future prospect.", J. Pharm. Pharmacol., 2013, 65, 634–51.

5. Du, Y. Q., Yang, X. X., Li, W. L., Wang, J. and Huang, C. Z., "A cancer-targeted drug delivery system developed with gold nanoparticle mediated DNA–doxorubicin conjugates", RSC Adv., 2014, 4, 34830.

6. Pandey, S., Oza, G., Mewada, A., Shah, R., Thakur, M. and Sharon, M., "Folic acid mediated synaphic delivery of doxorubicin using biogenic gold nanoparticles anchored to biological linkers", J. Mater. Chem., 2013, 9, 1361.

7. Qu, M., Mallidi, S., Mehrmohammadi, M., Truby, R., Homan, K., Joshi, P., Chen, Y. S., Sokolov, K. and Emelianov, S., "Magneto-photo-acoustic imaging", Biomed. Opt. Express., 2011, 2, 385.

8. Kim, S., Member, S., Chen, Y., Luke, G. P., Mehrmohammadi, M., Cook, J. R., "Ultrasound and Photoacoustic Image-guided Photothermal Therapy using Silica-coated Gold Nanorods : In-vivo Study", Proceedings of the Ultrasonic Symposium(IUS). IEEE, San Diego, USA, 2010, 233–236.

9. Guo, Y. J., Sun, G. M., Zhang, L., Tang, Y. J., Luo, J. J. and Yang, P. H., "Multifunctional optical probe based on gold nanorods for detection and identification of cancer cells", Sensors Actuators B Chem,. 2014, 191, 741–749.

10. Zhang, X., Li, D., Bourgeois, L., Wang, H., Webley, P. A., "Direct electrodeposition of porous gold nanowire arrays for biosensing applications.", Chemphyschem. 2009, 10, 436–41.

11. Nakao, H., Shiigi, H., Yamamoto, Y., Tokonami, S., Nagaoka, T., Sugiyama, S. and Ohtani, T., "Highly Ordered Assemblies of Au Nanoparticles Organized on DNA", Nano Lett., 2003, 3, 1391–1394.

12. Xue, Q., Jing, N., Chu, L., Ling, C. and Zhang, H., "Release of encapsulated molecules from carbon nanotubes using a displacing method: a MD simulation study", RSC Adv., 2012, 2, 6913.

13. Ju, S. P., "A molecular dynamics simulation of the adsorption of water molecules surrounding an Au nanoparticle.", J. Chem. Phys., 2005, 122, 094718.

14. Chang, C. I., Lee, W. J., Young, T. F., Ju, S. P., Chang, C. W., Chen, H. L. and Chang, J. G., "Adsorption mechanism of water molecules surrounding Au nanoparticles of different sizes.", J. Chem. Phys., 2008, 128, 154703.

15. Ju, S. P., Chang, J. G., Lin, J. S. and Lin, Y. S., "The effects of confinement on the behavior of water molecules between parallel Au plates of (001) planes.", J. Chem. Phys., 2005, 122, 154707.

16. Ju, S. P. and Chang, J. G., "A molecular dynamics simulation investigation into the behavior of water molecules inside Au nanotubes of various sizes", Microporous Mesoporous Mater. 2004, 75, 81–87.

17. Jorgensen, W. L., Chandrasekhar, J., Madura, J. D., Impey, R. W. and Klein, M. L., "Comparison of simple potential functions for simulating liquid water", J. Chem. Phys., 1983, 79, 926.

18. Jorgensen, W. L., "Quantum and statistical mechanical studies of liquids. 10. Transferable intermolecular potential functions for water, alcohols", and ethers. Application to liquid water, J. Am. Chem. Soc. 1981, 103, 335–340.

19. Hansen, J.P. and MacDonald, I.R., Theory of Simple Liquids, Second Edi, Academic Press, San Diego, USA, 1990, 149-199.

20. Rappe, A. K., Casewit, C. J., Colwell, K. S., Goddard, W. A. and Skiff, W. M., "UFF, a full periodic table force field for molecular mechanics and molecular dynamics simulations", J. Am. Chem. Soc., 1992, 114, 10024–10035.

21. Zwanzig, R.W., Kirkwood, J. G., Oppenheim, I. and Alder, B. J., "Statistical Mechanical Theory

of Transport Processes. VII. The Coefficient of Thermal Conductivity of Monatomic Liquids", J. Chem. Phys., 1954, 22, 783.

22. Leach, A. R., "Molecular Modelling: Principles and Applications", Second Edi, Prentice Hall, Dorchester, England, 2001, 410-454.

23. Allen, M. P. , Tildesley, D. J., "Computer Simulation of Liquids, Clarendon Press", Oxford, New York, USA, 1987, 198-208.

24. Hashemi Haeri, H., Ketabi, S. and Hashemianzadeh, S. M., "The solvation study of carbon, silicon and their mixed nanotubes in water solution.", J. Mol. Model., 2012, 18, 3379–88.